Published in final edited form as:
Biomaterials. 2011 August ; 32(22): 5241–5251. doi:10.1016/j.biomaterials.2011.03.063.

Effects of protein dose and delivery system on BMP-mediated bone regeneration

Joel D. Boerckel[1,2], **Yash M. Kolambkar**[1,3], **Kenneth M. Dupont**[1,2], **Brent A. Uhrig**[1,2], **Edward A. Phelps**[1,2], **Hazel Y. Stevens**[1,2], **Andrés J. García**[1,2], and **Robert E. Guldberg**[1,2,3]

Joel D. Boerckel: joel.boerckel@gatech.edu; Yash M. Kolambkar: yashk@gatech.edu; Kenneth M. Dupont: kennethmdupont@yahoo.com; Brent A. Uhrig: brent.uhrig@gatech.edu; Edward A. Phelps: eaphelps@gatech.edu; Hazel Y. Stevens: hazel.stevens@me.gatech.edu; Andrés J. García: andres.garcia@me.gatech.edu

[1] Parker H. Petit Institute for Bioengineering and Bioscience, Georgia Institute of Technology, 315 Ferst Dr. Atlanta, GA 30332, USA

[2] George W. Woodruff School of Mechanical Engineering, Georgia Institute of Technology, 315 Ferst Dr. Atlanta, GA 30332, USA

[3] Wallace H. Coulter Department of Biomedical Engineering, Georgia Institute of Technology, 315 Ferst Dr. Atlanta, GA 30332, USA

Abstract

Delivery of recombinant proteins is a proven therapeutic strategy to promote endogenous repair mechanisms and tissue regeneration. Bone morphogenetic protein-2 (rhBMP-2) has been used to promote spinal fusion and repair of challenging bone defects; however, the current clinically-used carrier, absorbable collagen sponge, requires high doses and has been associated with adverse complications. We evaluated the hypothesis that the relationship between protein dose and regenerative efficacy depends on delivery system. First, we determined the dose-response relationship for rhBMP-2 delivered to 8-mm rat bone defects in a hybrid nanofiber mesh/alginate delivery system at six doses ranging from 0 to 5 μg. Next, we directly compared the hybrid delivery system to the collagen sponge at 0.1 and 1.0 μg. Finally, we compared the *in vivo* protein release properties of the two delivery methods. In the hybrid delivery system, bone volume, connectivity and mechanical properties increased in a dose-dependent manner to rhBMP-2. Consistent bridging of the defect was observed for doses of 1.0 μg and greater. Compared to collagen sponge delivery at the same 1.0 μg dose, the hybrid system yielded greater connectivity by week 4 and 2.5-fold greater bone volume by week 12. These differences may be explained by the significantly greater protein retention in the hybrid system compared to collagen sponge. This study demonstrates a clear dose-dependent effect of rhBMP-2 delivered using a hybrid nanofiber mesh/alginate delivery system. Furthermore, the effective dose was found to vary with delivery system, demonstrating the importance of biomaterial carrier properties in the delivery of recombinant proteins.

Corresponding author: Phone# 404-894-6589; Fax# 404-385-1397, robert.guldberg@me.gatech.edu.

INTRODUCTION

Large bone defects associated with high-energy trauma, fracture nonunion, and bone tumor resection present a difficult challenge to orthopaedic surgeons accentuated by the limited effectiveness of current treatment options. The gold standard of care, the autograft, in which bone graft particles are surgically transplanted from the patient's iliac crest, is limited by the available volume of graft material and significant donor site morbidity [1–2]. Allografts are therefore often used to bridge the defects; however, these frequently fail to revascularize and remodel, resulting in graft fracture or tissue necrosis, requiring debridement and retreatment [3–5].

Biomaterials-mediated delivery of biologic agents including growth factors, stem cells, and genes has been used to stimulate regeneration of the structure and function of various tissues and has specifically emerged as a promising alternative to bone grafting techniques [6]. Delivery of recombinant proteins is a particularly attractive therapeutic strategy to promote endogenous repair mechanisms and tissue regeneration [6]. For a given protein, the delivery system may affect regenerative response by modulating protein stability and release kinetics. Langer and Folkman first demonstrated in 1976 the possibility of sustaining protein release via encapsulation in biocompatible polymers [7]. Since then, investigators have explored numerous materials and encapsulation and tethering techniques for tissue regenerative applications. For example, Griffith and colleagues have tethered growth factors to biomaterial substrates to regulate spatiotemporal presentation to mesenchymal stem cells and hepatocytes [8–10], and Phelps et al. covalently linked PEG hydrogels with vascular endothelial growth factor (VEGF) and cell adhesive peptides to enhance vascular network formation *in vivo* [11]. Others, such as Stayton and Mooney, have focused on modifying the degradation properties of various hydrogels to modulate growth factor delivery [12–13]. These inexhaustive examples illustrate the variety and power of the biomaterial delivery approach; however, degradation properties, release kinetics, and other material properties must be designed and tailored for each application [14–15].

Delivery of recombinant human osteoinductive growth factors is one of the most successful and clinically-applicable bone tissue engineering strategies to date [14]. The principle of bone induction dates back to Marshal Urist's seminal discovery in 1965 of the potential of devitalized, decalcified allografts to induce heterotopic bone formation [16]. Subsequently, Urist, Reddi, and others extracted and identified the active biological agents, the bone morphogenetic proteins (BMPs), which belong to the transforming growth factor-β (TGF-β) supergene family [17–22]. Identification of the genetic sequence of BMP-2 by Wozney and colleagues enabled production of highly purified BMPs through recombinant gene technology, which has facilitated its use as a clinical therapy [21, 23–25]. To date, two of the BMPs have been approved by the FDA for use in humans: BMP-2 and BMP-7, also known as human osteogenic protein-1 (hOP-1) [26].

Portending the tissue engineering paradigm in the early 1980's, Reddi and colleagues first isolated and combined these soluble osteoinductive factors with insoluble substrata to induce bone formation [17, 19]. This approach has seen continued success and aims to stimulate the endogenous regenerative potential of the host by recapitulating the molecular cascades that lead to bone formation during development [27–28]. However, as animal model and clinical data accumulate, the importance of the biomaterial carrier has become increasingly evident [26, 29], and while hOP-1 and rhBMP-2 have been successfully used in spinal fusion and open tibial fractures [30–34], significant limitations to current delivery systems remain [29]. In current clinical practice, rhBMP-2 is delivered by implanting an absorbable collagen sponge soaked in water-solubilized protein [29]. However, complications associated with rapid protein degradation and diffusion (such as soft tissue inflammation and ectopic bone

formation) [35–37], the cost of the high doses required for efficacy [38–42], and concerns over a correlation between extremely high doses of rhBMP-2 and cancer incidence [43] suggest that spatiotemporal delivery strategies may improve the efficacy, efficiency, and safety of recombinant growth factor delivery.

Of particular importance for growth factor delivery vehicles is the release profile of the protein from the scaffold, which must maintain a sufficient concentration to induce the desired response for a long enough time to promote recruitment of endogenous progenitor cells [14]. Development and assessment of such delivery vehicles requires systematic evaluation of protein dose-response relationships as well as comparison to the current clinical standard for both protein release and function. Such studies will facilitate comparison between different carrier systems, animal models, and associated protein doses.

The goal of this study was therefore to characterize and evaluate the dose-response of rhBMP-2 in a recently described protein delivery system designed to provide controlled spatial and temporal protein delivery [44], to compare this system with the clinically-used collagen sponge, and to explain the differences in response by quantifying the *in vivo* protein release profile of each. We hypothesized that bone regeneration responds in a dose-dependent manner to recombinant rhBMP-2 delivery in the nanofiber mesh/alginate delivery system and that this delivery system enhances bone regeneration over the currently used collagen sponge delivery method due to sustained protein release, thereby reducing the necessary effective dose.

MATERIALS AND METHODS

Surgical Procedure

Bilateral, critically-sized (8 mm) segmental defects were surgically created in femora of 13 week-old SASCO Sprague Dawley rats, as previously described [44–46]. Limbs were stabilized by custom radiolucent fixation plates that allowed *in vivo* monitoring with X-ray and microcomputed tomography (microCT). The experimental design featured 8 groups (Table 1, n = 9–10 per group). In 6 groups, the dose response of bone regeneration to rhBMP-2, when delivered in an alginate hydrogel, was evaluated at 0.0, 0.1, 0.5, 1.0, 2.5, and 5.0 μg rhBMP-2, respectively. In these groups, a nanofiber mesh tube was fitted over the bone ends, and RGD-functionalized alginate hydrogel [13] containing rhBMP-2 was injected into the defect space, as described previously [44]. In the remaining 2 groups, 0.1 and 1.0 μg soluble rhBMP-2 was adsorbed onto an 8 mm × 5 mm diameter collagen sponge, which was then press-fit into the defect. Post-surgery, animals were given subcutaneous injections of buprenorphine every 8 hours for three days. All procedures were approved by the Georgia Institute of Technology Institutional Animal Care and Use Committee (IACUC, protocol # A08032).

Nanofiber Mesh Production

Nanofiber meshes were produced as previously described [44]. Briefly, poly-(ε-caprolactone) (PCL) was dissolved at a concentration of 12% (w/v) in a 90:10 volume ratio of hexaflouro-2-propanol:dimethylformamide (Sigma-Aldrich) and electrospun onto a static collector. Twenty-four 1-mm diameter perforations were patterned into the nanofiber mesh sheets, which were then glued into tubes of 4.5 mm diameter and 12 mm length. Mesh tubes were sterilized by 100% ethanol evaporation, and were stored in sterile phosphate buffered saline (PBS) prior to implantation.

Alginate Gel & Collagen Sponge Growth Factor Loading

Recombinant human BMP-2 (R&D Systems) was reconstituted in 0.1% rat serum albumin in 4 mM HCl, according to manufacturer instructions. For the mesh/alginate delivery groups, the BMP-2 was then mixed at 6 different concentrations with RGD-functionalized alginate [13, 47] to a final concentration of 2% alginate, which was cross-linked by mixing rapidly with 0.84% (m/v) $CaSO_4$. Each defect received 200 μl of the pre-gelled alginate containing 0.0, 0.1, 0.5, 1.0, 2.5, or 5.0 μg rhBMP-2, depending on group. For the collagen sponge delivery groups, rhBMP-2 was pipetted onto the scaffolds 10 minutes prior to implantation at either 2 or 20 μg/ml, for the 0.1 and 1.0 μg groups, respectively.

Faxitron and MicroCT

Digital radiographs (Faxitron MX-20 Digital; Faxitron X-ray Corp.) were taken at 2, 4, 8, and 12 weeks post-surgery with an exposure time of 15 s and a voltage of 25 kV (n=10 per group). Bridging was defined by appearance of continuous bone crossing the defect. Bridging rates were blindly assessed by two independent observers, with differences determined by a third independent arbiter. At weeks 4, 8, and 12 post-surgery, animals were scanned using *in vivo* microCT (Viva-CT 40; Scanco Medical) at medium resolution and 38.5 μm isometric voxel size, with the scanner set at a voltage of 55 kVp and a current of 109 μA. The volume of interest (VOI) encompassed all bone formation within the center 120 slices (4.56 mm) between the native bone ends. New bone formation was segmented by application of a global threshold (386 mg hydroxylapatite/cm^3) corresponding to 50% of the native cortical bone density, and a Gaussian filter (sigma = 1.2, support = 1) was used to suppress noise.

Biomechanical Testing

After 12 weeks, animals were euthanized by CO_2 asphyxiation, and femora (n = 8–9 per group) were excised for biomechanical testing in torsion to failure as described previously [45]. Briefly, limbs were cleaned of soft tissues and the ends potted in Wood's metal (Alfa Aesar). The fixation plates were then removed, and limbs were mounted on a Bose ElectroForce system (ELF 3200, Bose EnduraTEC) and tested to failure at a rate of 3°/sec. Maximum torque at failure and torsional stiffness, given by the slope of the line fitted to the linear region of the torque-rotation curve, were computed for each sample.

Histology

One representative sample per group was taken for histology at week 12 post-surgery. Samples were chosen based on microCT-calculated average bone volume at week 8. Samples were fixed in 10% neutral buffered formalin for 48 hours at 4°C and then transferred to a formic acid-based decalcifier (Cal-ExII, Fisher Scientific) for 2 weeks under mild agitation on a rocker plate. Following paraffin processing, 5 μm-thick mid-saggital sections were cut and stained with Safranin-O/Fast-green [48] and Haematoxylin and Eosin (H&E). Due to the presence of carboxyl groups, alginate carries a negative charge [49], allowing high contrast staining with Safranin-O.

BMP-2 Tracking

A separate study was conducted to compare the protein release and degradation over time *in vivo*. Segmental defects were created as described above and were treated with 2.5 μg near-infrared (NIR) fluorophore-tagged rhBMP-2, delivered in either collagen sponge or nanofiber mesh/alginate. rhBMP-2 was tagged with an *in vivo* NIR fluorochrome label (VivoTag-S 750, VisEn Medical) using NHS-ester chemistry. Briefly, rhBMP-2 was reconstituted in 4 mM HCl at a concentration of 100 μg/ml. Due to presence of glycine in the lyophilization buffer, the buffer was exchanged to 100 mM $NaPO_4$ at pH 7.5 by two

rounds of filtration through a 3 kDa centrifugal filter (Millipore Amicon Ultra, Millipore). The protein was then labeled by 4 hour incubation with 6 M excess of the fluorophore at room temperature. Excess fluorophore was removed by gel filtration through Zeba Spin Desalting Columns (7K MWCO, Fisher Scientific). Protein tagging was verified by SDS-PAGE (S-Figure 3). Labeled protein fluorescence was tracked over 21 days *in vivo* using a 700 series Xenogen IVIS Imaging System. Animals were imaged at 745 nm excitation, 780 nm emission and 60 s exposure time at 0, 3, 7, 14, and 21 days post-surgery. Fluorescence intensity was measured as background-subtracted average efficiency within a fixed region of interest (ROI) centered on the defect site. Values from each sample were normalized to that sample's initial intensity to represent percentage of protein remaining [15, 50]. Nonlinear regression analysis of release profiles were performed on raw data in GraphPad Prism using a one-phase exponential decay model (GraphPad Software, Inc.).

Statistical Analyses

All data are presented as mean ± standard error of the mean (SEM). Differences between groups and among time points were assessed by analysis of variance (ANOVA) with pairwise comparisons made by Tukey's post hoc analysis, Chi-squared analysis with individual comparisons made by Fisher's Exact test, analysis of covariance (ANCOVA) and Student's t-test, where appropriate ($\alpha = 0.05$). A natural log transformation was applied to maintain normality of residuals and homogeneity of variance, when necessary and appropriate. Minitab® 15 (Minitab, Inc.) was used to perform the statistical analysis.

RESULTS: DOSE-DEPENDENCY

First, the dose response of rhBMP-2 in the nanofiber mesh/alginate delivery system was evaluated over 12 weeks in critically-sized rat femoral bone defects.

Faxitron

In vivo digital radiographs (Figure 1A) qualitatively demonstrated a dose-dependent bone formation response to rhBMP-2, and longitudinal evaluation of bridging rates likewise revealed significant dose-dependency of defect bridging to amount of rhBMP-2 delivered using the mesh/alginate system (Table 2). Groups with 1.0 μg rhBMP-2 or greater achieved consistent (80–100%) bridging by week 12 post-surgery. Doses less than or equal to 0.5 μg rhBMP-2 failed to bridge consistently.

Microcomputed Tomography

MicroCT scans confirmed the two-dimensional X-ray results. Minimal bone formation occurred at low doses. Beginning at the 0.5 μg dose, however, bone formation was evident at the center of the defects as well as on the surfaces of the nanofiber mesh, where the holes in the newly-formed bone corresponded with mesh perforations (Figure 1B). Local density maps on saggital cross sections demonstrated the distribution and maturity of bone within the defects (Figure 1B). At doses higher than 1.0 μg, bone formed throughout the defects, with dose-dependent increases in defect filling.

MicroCT was used to quantify 3D tissue ingrowth parameters including volume, density, and connectivity of the newly formed bone. In the mesh/alginate groups, bone formation responded in a nonlinear, dose-dependent manner to rhBMP-2. By week 12, the 1.0 and 2.5 μg doses had significantly greater bone volume than 0.0, 0.1, and 0.5 μg doses, and the 5.0 μg dose group exhibited significantly greater bone volume than all other groups (Figure 2A). The dose-response curve exhibited linear biphasic behavior, with the slope (m_bv) of the bone volume vs. dose curve decreasing significantly ($p < 0.0001$) at 1.0 μg or greater ($m\_bv_{0.0–1.0} = 50.1 \pm 4.8$ mm^3/μg and $m\_bv_{1.0–5.0} = 9.21 \pm 2.8$ mm^3/μg, $R^2 = 0.75$ and

0.30, respectively, at week 12). There were no differences in mean mineral density among the dose groups at any time point, though the density increased with time for all groups (S-Figure 1A). Connectivity increased with rhBMP-2 dose in a similar manner to bone volume. However, unlike bone volume, the connectivity of the bone microstructure decreased with time as the initial finely-trabeculated structure was remodeled between 4 and 12 weeks (Figure 2B).

Biomechanical Testing

To evaluate the degree of functional restoration, biomechanical testing in torsion to failure was performed on potted femurs. Biomechanical properties increased continuously with increasing dose of rhBMP-2, with the 1.0, 2.5, and 5.0 μg groups having significantly greater torsional stiffness (Figure 2C) and maximum torque at failure (Figure 2D) than the 0.0, 0.1, and 0.5 μg groups. In contrast to bone volume and connectivity, which featured a reduction in response to increasing dose at doses greater than 1.0 μg rhBMP-2, mechanical properties exhibited continuously increasing stiffness and torque with increasing protein dose, and the dose-response curves did not significantly change slope over the range of doses evaluated ($p = 0.47$ and $p = 0.65$ for stiffness and torque, respectively).

Histology

Histological staining allowed evaluation of tissue morphology, cellular infiltration, and alginate gel degradation at week 12. Haematoxylin and Eosin staining revealed a mixture of osteocyte-populated woven and lamellar bone in groups with bone formation (Figure 3A, S-Figure 2). In the 0.0 μg group, the defect space appeared highly homogeneous and filled with alginate gel. In this group, very few cells had migrated into the defect space, and tissue invasion into the alginate was minimal. In contrast, large numbers of invading cells were present in all other groups, even at very low doses of BMP, though cellular infiltration appeared to increase in a dose-dependent manner. The degree of fragmentation of the alginate gel was found through

Safranin-O/fast green staining to likewise be dose-dependent, featuring negligible dissolution in the 0.0 μg group and increased tissue invasion and alginate fragmentation with increasing amounts of rhBMP-2 (Figure 3B). Regardless of protein dose, the gel did not completely degrade by 12 weeks, as indicated by the presence of small regions of alginate embedded in mineralized matrix even at the 5 μg dose.

RESULTS: DELIVERY SYSTEM COMPARISON

Next, we compared the nanofiber mesh/alginate delivery system at a non-bridging dose (0.1 μg) and a bridging dose (1.0 μg) with the clinically-used collagen sponge delivery system at the same doses. Finally, we compared the *in vivo* protein release kinetics of the two delivery methods using fluorophore-tagged rhBMP-2.

Faxitron

In vivo digital radiographs (Figure 4A) qualitatively demonstrated a delivery system-dependent bone formation response to rhBMP-2. At 1.0 μg rhBMP-2, the mesh/alginate delivery system resulted in 100% defect bridging by week 12, while collagen sponge delivery resulted in 60% bridging, though this difference was not statistically significant with $p = 0.0867$ (Table 3). 0.1 μg rhBMP-2 was insufficient to induce robust bone formation in either delivery system.

Microcomputed Tomography

MicroCT scans again confirmed the two-dimensional X-ray results and clearly illustrated differences in delivery systems at 1.0 μg rhBMP-2 (Figure 4B). Local density maps on saggital cross sections demonstrated the distribution and maturity of bone within the defects (Figure 4B). Collagen groups exhibited formation of thin bony shells containing small amounts of trabeculated bone, while the mesh/alginate group featured bone formation throughout the defect at 1.0 μg.

Quantification of microCT images revealed significant differences in bone formation between the collagen sponge and mesh/alginate delivery systems (Figure 5A–F). At week 4, there were no differences in bone volume between groups at either 0.1 or 1.0 μg dose (Figure 5A). However, by week 8, the bone volume in the mesh/alginate 1.0 μg group was significantly greater than the collagen sponge 1.0 μg group, and this effect widened to 2.5-fold greater by week 12 (Figure 5C, E). Temporally, bone volume increased significantly from week 4 to weeks 8 and 12 with mesh/alginate delivery, whereas with collagen sponge delivery, bone formation occurred rapidly over the first 4 weeks but did not increase significantly after week 4. As among the mesh/alginate groups, no differences in mean mineral density were found between groups, though the density increased with time in each group (S-Figure 1B–D). Connectivity was significantly greater in the mesh/alginate 1.0 μg group than the collagen sponge 1.0 μg group at both weeks 4 and 8 (Figure 5D, E); however, by week 12, the connectivity had normalized in both groups (Figure 5F). No differences in bone formation were found between collagen and mesh/alginate delivery at the low dose of 0.1 μg at any time point for any measure (Figure 5).

Biomechanical Testing

Differences in torsional stiffness and maximum torque did not reach significance between collagen and mesh/alginate delivery, $p = 0.057$ and $p = 0.082$, respectively (Figure 5G, H).

Histology

Histological staining with H&E and Safranin-O/fast green was performed to compare tissue morphology and composition between delivery systems at week 12 (Figure 6). In contrast to the mesh/alginate groups which contained regions of non-degraded hydrogel through week 12, the collagen sponges had completely resorbed. In the collagen sponge 0.1 μg group, defects were filled primarily with fibrous tissue, while in the collagen sponge 1.0 μg group, the new bone formed thin shells, containing trabeculated bone and marrow.

BMP Release

To investigate a possible mechanism for the observed delivery system-dependent increases in bone formation, fluorescently-labeled protein was tracked over 3 weeks (Figure 7). For both delivery systems, the labeled protein profile decreased monotonically with time and >90% of the initial dose delivered was released by 21 days. The percentage of protein remaining in the defect region was significantly elevated in the mesh/alginate group compared to collagen sponge at both 3 and 7 days post-implantation. Based on a simple release model, the protein profiles were fit to an exponential decay to estimate the half-life of release ($R^2 = 0.946$ and 0.857 for collagen sponge and mesh/alginate groups, respectively). Overall, the half-life of release was 1.87 days (95% CI: 1.49 – 2.49 days) and 3.19 days (95% CI: 2.23 – 5.59 days) for the collagen sponge and mesh/alginate, respectively, though the difference did not reach statistical significance with $p = 0.094$. No significant differences in spatial distribution were found between the groups at any time point (data not shown). SDS-PAGE analysis verified that the tagged protein had similar molecular weight to the untagged protein (S-Figure 3). *In vitro* bioactivity assays and bone

formation *in vivo* demonstrated that the tagged rhBMP-2 maintained biofunctionality, capable of inducing osteogenic differentiation of mesenchymal stem cells to a similar degree as un-tagged protein, as measured by calcium deposition (S-Figure 4A), though tagged protein induced a lesser amount of bone formation *in vivo* suggesting a somewhat reduced activity (S-Figure 4B).

DISCUSSION

Delivery of recombinant proteins carries great promise for the field of regenerative medicine; however, optimal doses and delivery vehicles have not yet been determined. This study presents the dose-response relationships for rhBMP-2 delivered in a controlled-release hydrogel in comparison to the currently-used collagen sponge carrier, and revealed a reduction in the necessary effective dose for the spatiotemporal delivery system.

Dose-dependency

When delivered in the nanofiber mesh/alginate delivery system, rhBMP-2 induced bone regeneration in a nonlinear dose-dependent manner, as evaluated by bridging rate, bone volume, connectivity, and mechanical properties. Interestingly, the dose-response curves for bone volume and connectivity exhibited linear biphasic characteristics, with the slope significantly decreasing after the onset of bridging at 1.0 μg. This decrease in responsiveness to rhBMP-2 with increasing dose is likely due to saturation of BMP receptors and responding cell supply or simply from bone filling up available space in the defect region. Consistent with the onset of defect bridging, torsional stiffness and strength were not dose-responsive at less than 1.0 μg, but at higher doses, exhibited significant dose-dependent increases in mechanical properties.

The observation that mechanical properties did not level off within the range of growth factor dose analyzed may be explained by the histological observation that alginate degradation also proceeded in a dose-dependent manner, such that at higher doses, increased gel degradation allowed improved mechanical integrity. Since alginate is algae-derived, it cannot be enzymatically degraded *in vivo*, requiring hydrolysis or loss of the cross-linking Ca^{2+} ions for degradation [13]. The observed increase in cell and tissue infiltration with increasing dose may have increased the number of cells responsible for clearing foreign material and exposed more of the alginate surface for hydrolysis, contributing to the dose-dependence of gel degradation.

Another possible explanation is that the presence of the rhBMP-2 in the gel directly affected mechanical properties or degradation profiles independent of cellular and tissue interactions. Together, these effects allowed increased mechanical integrity in the higher doses which contained more bone and lower amounts of residual hydrogel.

For comparison, the mechanical properties of age-matched intact femurs were 0.030 ± 0.001 N-m/deg and 0.31 ± 0.02 N-m for torsional stiffness and failure torque, respectively [46]. At the 5.0 μg dose, the torsional stiffness of the regenerated defects exceeded the intact bone stiffness, while the failure torque reached about 60% of that of the intact bone. A previous study using this model demonstrated similar results, with mesh/alginate delivery of 5 μg rhBMP-2 reaching about 75% of intact bone properties for both stiffness and torque, though these were not statistically different from the native bone properties [44].

Delivery System Comparison

Bone formation was significantly increased in the nanofiber mesh/alginate delivery system over the current clinically-used collagen sponge delivery method for the 1.0 μg groups. Although the amount of bone formation was similar at week 4, by week 8 there was

significantly greater bone volume in the mesh/alginate group compared to the collagen sponge group, and this difference increased through week 12. By week 4, the amount of active rhBMP-2 remaining in the defect would likely be minimal for both groups, however, this enhancement in bone formation between week 4 and week 8 in the mesh/alginate system may be attributed to an increased attraction of cells into the defect at earlier time points or enhanced activation of those cells from the released rhBMP-2, resulting in elevated activity through week 8. 0.1 μg rhBMP-2 was not sufficient to induce robust bone formation; however, 0.1 μg caused substantial increases in cellular migration into the defect compared to mesh/alginate-only treatment, demonstrating that even a low dose of rhBMP-2 possesses potent chemoattractant capacity for endogenous cells [51] and suggesting that low doses of rhBMP-2 may be useful for combination strategies involving gene therapy or growth factor co-delivery which require a strong host cell response. To facilitate cellular invasion, the alginate gel was functionalized with RGD peptides. RGD (Arg-Gly-Asp) is the primary sequence motif of fibronectin responsible for integrin binding, and may have enhanced protein-cell-matrix interactions and the ability of cells to migrate into the defect [13]. The RGD alone was not sufficient to induce cellular invasion or gel dissolution, as evident in the 0.0 μg group, though cellular infiltration and associated gel fragmentation increased in an rhBMP-2 dose-dependent manner.

Although early bone formation occurred at a similar rate between delivery systems, an early enhancement in connectivity was observed in the mesh/alginate group, and this difference persisted through week 8. In both delivery systems, however, the connectivity decreased with time, despite increasing with dose of rhBMP-2, resulting in similar connectivity at week 12. As connectivity is a normalized measure of the number of redundant structures, the dose-dependent increase may be explained by an increase in the number of bone nucleation sites. However, as time progressed, spaces between distinct islands of bone filled in, reducing the total number of unique structures within the defect space, causing a reduction in connectivity over time, though the actual integrity increased.

Differences in mechanical properties between the collagen and mesh/alginate systems did not reach statistical significance, though the trends were consistent with the observed differences in bone formation. As seen histologically, the alginate hydrogel did not fully degrade over the time course of the study, and the extant alginate gel may have interfered with the mechanical integrity of the resulting bone by preventing complete interconnectivity. This underscores the importance of optimizing carrier degradation kinetics and protein-carrier concentrations for effective sustained delivery.

To explain the differences in bone formation between the two delivery systems, we quantified the *in vivo* protein release profiles of each. Sustained delivery vehicles for recombinant proteins have been studied previously, primarily using ^{125}I-labeled proteins [15, 50, 52–57]. In this study, the protein release kinetics from the collagen sponge were similar to those reported previously in ectopic bone formation models, in which the retention half-life ranged from several hours to several days [58–61]. In comparison to collagen sponge, the sustained delivery method examined here increased the protein retention, and resulted in a 2.5-fold increase in bone volume over collagen sponge delivery.

A possible limitation of the protein tagging technique is that the fluorophore attachment may have altered the release properties of the protein. However, since the protein was not substantially changed in size as a result of complexation and did maintain bioactivity, albeit somewhat reduced *in vivo* compared to un-tagged protein, it is likely that the diffusion properties were not substantially changed. Regardless, both collagen sponge and mesh/alginate delivery systems were analyzed with the same tagged protein, allowing direct comparison. As with all protein labeling techniques, the entity being tracked is the

fluorophore, with the degree of fluorophore-protein dissociation an unknown. Dissociation would result in measurement of faster release kinetics than actually exist as the fluorophore is substantially smaller in size than the fluorophore-protein complex, resulting in greater diffusivity according to the Einstein-Stokes relation. However, in this experiment, both groups received the same labeled protein, processed identically, and the fluorophore-protein dissociation rate is not likely to differ between delivery systems. Together, these limitations accentuate the importance of including the collagen group when evaluating sustained delivery vehicles for recombinant proteins to provide direct comparison of the novel therapeutic with the clinical standard.

In this study, several combined factors may have prolonged the protein release in the mesh/alginate system. First, the alginate hydrogel mesh structure provides a diffusional barrier to BMP release, whereas the collagen sponge relies mostly on desorption. Second, the slow degradation kinetics of the alginate gel, despite inhibiting whole bone remodeling, may have contributed to the slower release kinetics. Third, the presence of the nanofiber mesh tube has been shown to maintain spatial retention of alginate in the defect [44] and may contribute to protein retention as well. Finally, since alginate carries a negative charge [62], and rhBMP-2 carries a positive charge of 10.5 at pH 7.4 [63], the opposite protein-matrix charge interactions may also have contributed to protein retention. Specifically, alginate has been shown to reversibly bind to heparin-binding proteins such as BMP-2 due to the abundance of basic residues in the heparin binding sequence, promoting interaction with negatively charged carboxyl groups on the alginate chain [64–65]. This interaction has been shown to enhance the biological activity of these proteins, likely through protection from degradation [55].

Much attention has recently been placed on developing improved carriers for both rhBMP-2 and hOP-1 [15, 66–67]. Likewise, the kinetics of protein release have been shown to have profound effects on protein effectiveness and efficiency [15, 50]. For example, Li et al. evaluated the bone formation capacity of rhBMP-2 when delivered in polyurethane scaffolds possessing different release kinetics, and found improved healing in scaffolds featuring an initial burst followed by sustained release [68]. Subsequently, Brown et al. demonstrated that a burst followed by a sustained release of rhBMP-2 regenerated 50% more bone compared to collagen sponge [69]. These results suggest that some amount of early release combined with sustained delivery may enhance growth factor efficacy, and together with the present data emphasize the importance of spatiotemporal growth factor presentation in tissue-engineered bone regeneration.

CONCLUSIONS

These data demonstrate the dose-response and temporal release of rhBMP-2 in a spatiotemporal protein delivery system, in comparison to the clinical standard collagen sponge. This work demonstrates an improvement in bone formation over current rhBMP-2 delivery methods, and highlights the importance of quantification of release kinetics and scaffold degradation properties for evaluating novel recombinant protein carriers.

Supplementary Material

Refer to Web version on PubMed Central for supplementary material.

Acknowledgments

Funding Source: This study was supported by grants from the NIH, AFIRM, and DoD.

This work was supported by grants from the NIH (R01 AR051336), AFIRM, and DoD. The authors would like to thank the following individuals: Dr. David Mooney, for providing the RGD-alginate and Dr. Laura O'Farrell, for assistance with animal studies. We gratefully acknowledge Angela Lin, Dr. Tamim Diab, Dr. Mela Johnson, Christopher Dosier, Jessica O'Neal, Jason Wang, Tanushree Thote, Alice Li, and Ashley Allen for their assistance in surgeries.

References

1. Sasso RC, LeHuec JC, Shaffrey C. Iliac crest bone graft donor site pain after anterior lumbar interbody fusion: a prospective patient satisfaction outcome assessment. J Spinal Disord Tech. 2005; 18(Suppl):S77–81. [PubMed: 15699810]
2. Rihn JA, Kirkpatrick K, Albert TJ. Graft options in posterolateral and posterior interbody lumbar fusion. Spine (Phila Pa 1976). 2010; 3517:1629–1639. [PubMed: 20628336]
3. Koefoed M, Ito H, Gromov K, Reynolds DG, Awad HA, Rubery PT, et al. Biological effects of rAAV-caAlk2 coating on structural allograft healing. Mol Ther. 2005; 122:212–218. [PubMed: 16043092]
4. Berrey BH Jr, Lord CF, Gebhardt MC, Mankin HJ. Fractures of allografts. Frequency, treatment, and end-results. J Bone Joint Surg Am. 1990; 726:825–833. [PubMed: 2365716]
5. Zhang X, Awad HA, O'Keefe RJ, Guldberg RE, Schwarz EM. A perspective: engineering periosteum for structural bone graft healing. Clin Orthop Relat Res. 2008; 4668:1777–1787. [PubMed: 18509709]
6. Guldberg RE. Spatiotemporal delivery strategies for promoting musculoskeletal tissue regeneration. J Bone Miner Res. 2009; 249:1507–1511. [PubMed: 19653806]
7. Langer R, Folkman J. Polymers for the sustained release of proteins and other macromolecules. Nature. 1976; 2635580:797–800. [PubMed: 995197]
8. Mehta G, Williams CM, Alvarez L, Lesniewski M, Kamm RD, Griffith LG. Synergistic effects of tethered growth factors and adhesion ligands on DNA synthesis and function of primary hepatocytes cultured on soft synthetic hydrogels. Biomaterials. 2010; 3117:4657–4671. [PubMed: 20304480]
9. Platt MO, Roman AJ, Wells A, Lauffenburger DA, Griffith LG. Sustained epidermal growth factor receptor levels and activation by tethered ligand binding enhances osteogenic differentiation of multi-potent marrow stromal cells. J Cell Physiol. 2009; 2212:306–317. [PubMed: 19544388]
10. Fan VH, Tamama K, Au A, Littrell R, Richardson LB, Wright JW, et al. Tethered epidermal growth factor provides a survival advantage to mesenchymal stem cells. Stem Cells. 2007; 255:1241–1251. [PubMed: 17234993]
11. Phelps EA, Landazuri N, Thule PM, Taylor WR, Garcia AJ. Bioartificial matrices for therapeutic vascularization. Proc Natl Acad Sci U S A. 2010; 1078:3323–3328. [PubMed: 20080569]
12. Patterson J, Siew R, Herring SW, Lin AS, Guldberg R, Stayton PS. Hyaluronic acid hydrogels with controlled degradation properties for oriented bone regeneration. Biomaterials. 2010; 3126:6772–6781. [PubMed: 20573393]
13. Simmons CA, Alsberg E, Hsiong S, Kim WJ, Mooney DJ. Dual growth factor delivery and controlled scaffold degradation enhance in vivo bone formation by transplanted bone marrow stromal cells. Bone. 2004; 352:562–569. [PubMed: 15268909]
14. Seeherman H, Wozney J, Li R. Bone morphogenetic protein delivery systems. Spine (Phila Pa 1976). 2002; 2716(Suppl 1):S16–23. [PubMed: 12205414]
15. Kempen DH, Yaszemski MJ, Heijink A, Hefferan TE, Creemers LB, Britson J, et al. Non-invasive monitoring of BMP-2 retention and bone formation in composites for bone tissue engineering using SPECT/CT and scintillation probes. J Control Release. 2009; 1343:169–176. [PubMed: 19105972]
16. Urist MR. Bone: formation by autoinduction. Science. 1965; 150698:893–899. [PubMed: 5319761]
17. Sampath TK, Reddi AH. Homology of bone-inductive proteins from human, monkey, bovine, and rat extracellular matrix. Proc Natl Acad Sci U S A. 1983; 8021:6591–6595. [PubMed: 6579546]

18. Sampath TK, Muthukumaran N, Reddi AH. Isolation of osteogenin, an extracellular matrix-associated, bone-inductive protein, by heparin affinity chromatography. Proc Natl Acad Sci U S A. 1987; 8420:7109–7113. [PubMed: 3478684]
19. Sampath TK, Reddi AH. Dissociative extraction and reconstitution of extracellular matrix components involved in local bone differentiation. Proc Natl Acad Sci U S A. 1981; 7812:7599–7603. [PubMed: 6950401]
20. Urist MR, Strates BS. Bone morphogenetic protein. J Dent Res. 1971; 506:1392–1406. [PubMed: 4943222]
21. Wozney JM, Rosen V, Celeste AJ, Mitsock LM, Whitters MJ, Kriz RW, et al. Novel regulators of bone formation: molecular clones and activities. Science. 1988; 2424885:1528–1534. [PubMed: 3201241]
22. Urist MR, Mikulski A, Lietze A. Solubilized and insolubilized bone morphogenetic protein. Proc Natl Acad Sci U S A. 1979; 764:1828–1832. [PubMed: 221908]
23. Lieberman JR, Daluiski A, Einhorn TA. The role of growth factors in the repair of bone. Biology and clinical applications. J Bone Joint Surg Am. 2002; 84-A6:1032–1044. [PubMed: 12063342]
24. Jones AL, Bucholz RW, Bosse MJ, Mirza SK, Lyon TR, Webb LX, et al. Recombinant human BMP-2 and allograft compared with autogenous bone graft for reconstruction of diaphyseal tibial fractures with cortical defects. A randomized, controlled trial. J Bone Joint Surg Am. 2006; 887:1431–1441. [PubMed: 16818967]
25. Riley EH, Lane JM, Urist MR, Lyons KM, Lieberman JR. Bone morphogenetic protein-2: biology and applications. Clin Orthop Relat Res. 1996; 324:39–46. [PubMed: 8595775]
26. Einhorn TA. Clinical applications of recombinant human BMPs: early experience and future development. J Bone Joint Surg Am. 2003; 85-A(Suppl 3):82–88. [PubMed: 12925614]
27. Ebara S, Nakayama K. Mechanism for the action of bone morphogenetic proteins and regulation of their activity. Spine (Phila Pa 1976). 2002; 2716(Suppl 1):S10–15. [PubMed: 12205413]
28. Minear S, Leucht P, Miller S, Helms JA. rBMP represses Wnt signaling and influences skeletal progenitor cell fate specification during bone repair. J Bone Miner Res. 2010; 256:1196–1207. [PubMed: 20200943]
29. Bessa PC, Casal M, Reis RL. Bone morphogenetic proteins in tissue engineering: the road from laboratory to clinic, part II (BMP delivery). J Tissue Eng Regen Med. 2008; 22–3:81–96.
30. Boden SD, Kang J, Sandhu H, Heller JG. Use of recombinant human bone morphogenetic protein-2 to achieve posterolateral lumbar spine fusion in humans: a prospective, randomized clinical pilot trial: 2002 Volvo Award in clinical studies. Spine (Phila Pa 1976). 2002; 2723:2662–2673. [PubMed: 12461392]
31. McKay B, Sandhu HS. Use of recombinant human bone morphogenetic protein-2 in spinal fusion applications. Spine (Phila Pa 1976). 2002; 2716(Suppl 1):S66–85. [PubMed: 12205423]
32. Johnsson R, Stromqvist B, Aspenberg P. Randomized radiostereometric study comparing osteogenic protein-1 (BMP-7) and autograft bone in human noninstrumented posterolateral lumbar fusion: 2002 Volvo Award in clinical studies. Spine (Phila Pa 1976). 2002; 2723:2654–2661. [PubMed: 12461391]
33. Vaccaro AR, Patel T, Fischgrund J, Anderson DG, Truumees E, Herkowitz HN, et al. A pilot study evaluating the safety and efficacy of OP-1 Putty (rhBMP-7) as a replacement for iliac crest autograft in posterolateral lumbar arthrodesis for degenerative spondylolisthesis. Spine (Phila Pa 1976). 2004; 2917:1885–1892. [PubMed: 15534410]
34. Kanayama M, Hashimoto T, Shigenobu K, Yamane S, Bauer TW, Togawa D. A prospective randomized study of posterolateral lumbar fusion using osteogenic protein-1 (OP-1) versus local autograft with ceramic bone substitute: emphasis of surgical exploration and histologic assessment. Spine (Phila Pa 1976). 2006; 3110:1067–1074. [PubMed: 16648739]
35. Cahill KS, Chi JH, Day A, Claus EB. Prevalence, complications, and hospital charges associated with use of bone-morphogenetic proteins in spinal fusion procedures. JAMA. 2009; 3021:58–66. [PubMed: 19567440]
36. Benglis D, Wang MY, Levi AD. A comprehensive review of the safety profile of bone morphogenetic protein in spine surgery. Neurosurgery. 2008; 625(Suppl 2):ONS423–431. discussion ONS431. [PubMed: 18596525]

37. Paramore CG, Lauryssen C, Rauzzino MJ, Wadlington VR, Palmer CA, Brix A, et al. The safety of OP-1 for lumbar fusion with decompression-- a canine study. Neurosurgery. 1999; 445:1151–1155. discussion 1155–1156. [PubMed: 10232555]
38. Garrison KR, Donell S, Ryder J, Shemilt I, Mugford M, Harvey I, et al. Clinical effectiveness and cost-effectiveness of bone morphogenetic proteins in the non-healing of fractures and spinal fusion: a systematic review. Health Technol Assess. 2007; 1130:1–150. iii–iv. [PubMed: 17669279]
39. Visser R, Arrabal PM, Becerra J, Rinas U, Cifuentes M. The effect of an rhBMP-2 absorbable collagen sponge-targeted system on bone formation in vivo. Biomaterials. 2009; 3011:2032–2037. [PubMed: 19155065]
40. Geiger M, Li RH, Friess W. Collagen sponges for bone regeneration with rhBMP-2. Adv Drug Deliv Rev. 2003; 5512:1613–1629. [PubMed: 14623404]
41. Swiontkowski MF, Aro HT, Donell S, Esterhai JL, Goulet J, Jones A, et al. Recombinant human bone morphogenetic protein-2 in open tibial fractures. A subgroup analysis of data combined from two prospective randomized studies. J Bone Joint Surg Am. 2006; 886:1258–1265. [PubMed: 16757759]
42. Dahabreh Z, Calori GM, Kanakaris NK, Nikolaou VS, Giannoudis PV. A cost analysis of treatment of tibial fracture nonunion by bone grafting or bone morphogenetic protein-7. Int Orthop. 2009; 335:1407–1414. [PubMed: 19052743]
43. Orthopaedic and Rehabilitation Devices Advisory Panel, USFaDA. Executive Summary for P050036 Medtronic's AMPLIFY rhBMP-2 Matrix. 2010.
44. Kolambkar YM, Dupont KM, Boerckel JD, Huebsch N, Mooney DJ, Hutmacher DW, et al. An alginate-based hybrid system for growth factor delivery in the functional repair of large bone defects. Biomaterials. 2011; 321:65–74. [PubMed: 20864165]
45. Oest ME, Dupont KM, Kong HJ, Mooney DJ, Guldberg RE. Quantitative assessment of scaffold and growth factor-mediated repair of critically sized bone defects. J Orthop Res. 2007
46. Boerckel JD, Dupont KM, Kolambkar YM, Lin AS, Guldberg RE. In vivo model for evaluating the effects of mechanical stimulation on tissue-engineered bone repair. J Biomech Eng. 2009; 1318:084502. [PubMed: 19604025]
47. Alsberg E, Kong HJ, Hirano Y, Smith MK, Albeiruti A, Mooney DJ. Regulating bone formation via controlled scaffold degradation. J Dent Res. 2003; 8211:903–908. [PubMed: 14578503]
48. Rosenberg L. Chemical basis for the histological use of safranin O in the study of articular cartilage. J Bone Joint Surg Am. 1971; 531:69–82. [PubMed: 4250366]
49. You JO, Park SB, Park HY, Haam S, Chung CH, Kim WS. Preparation of regular sized Ca-alginate microspheres using membrane emulsification method. J Microencapsul. 2001; 184:521–532. [PubMed: 11428680]
50. Kempen DH, Lu L, Classic KL, Hefferan TE, Creemers LB, Maran A, et al. Non-invasive screening method for simultaneous evaluation of in vivo growth factor release profiles from multiple ectopic bone tissue engineering implants. J Control Release. 2008; 1301:15–21. [PubMed: 18554743]
51. LI M, Eriksen EF, Bunger C. Bone morphogenetic protein-2 but not bone morphogenetic protein-4 and -6 stimulates chemotactic migration of human osteoblasts, human marrow osteoblasts, and U2-OS cells. Bone. 1996; 181:53–57.
52. Ruhe PQ, Boerman OC, Russel FG, Spauwen PH, Mikos AG, Jansen JA. Controlled release of rhBMP-2 loaded poly(dl-lactic-co-glycolic acid)/calcium phosphate cement composites in vivo. J Control Release. 2005; 1061–2:162–171.
53. Delgado JJ, Evora C, Sanchez E, Baro M, Delgado A. Validation of a method for non-invasive in vivo measurement of growth factor release from a local delivery system in bone. J Control Release. 2006; 1142:223–229. [PubMed: 16859798]
54. Yamamoto M, Takahashi Y, Tabata Y. Controlled release by biodegradable hydrogels enhances the ectopic bone formation of bone morphogenetic protein. Biomaterials. 2003; 2424:4375–4383. [PubMed: 12922150]

55. Peters MC, Isenberg BC, Rowley JA, Mooney DJ. Release from alginate enhances the biological activity of vascular endothelial growth factor. J Biomater Sci Polym Ed. 1998; 912:1267–1278. [PubMed: 9860169]
56. Ruhe PQ, Boerman OC, Russel FG, Mikos AG, Spauwen PH, Jansen JA. In vivo release of rhBMP-2 loaded porous calcium phosphate cement pretreated with albumin. J Mater Sci Mater Med. 2006; 1710:919–927. [PubMed: 16977389]
57. Woo BH, Fink BF, Page R, Schrier JA, Jo YW, Jiang G, et al. Enhancement of bone growth by sustained delivery of recombinant human bone morphogenetic protein-2 in a polymeric matrix. Pharm Res. 2001; 1812:1747–1753. [PubMed: 11785696]
58. Uludag H, Gao T, Porter TJ, Friess W, Wozney JM. Delivery systems for BMPs: factors contributing to protein retention at an application site. J Bone Joint Surg Am. 2001; 83-A(Suppl 1Pt 2):S128–135. [PubMed: 11314790]
59. Wang Y, Zhang L, Hu M, Wen W, Xiao H, Niu Y. Effect of chondroitin sulfate modification on rhBMP-2 release kinetics from collagen delivery system. J Biomed Mater Res A. 2010; 922:693–701. [PubMed: 19263491]
60. Friess W, Uludag H, Foskett S, Biron R, Sargeant C. Characterization of absorbable collagen sponges as recombinant human bone morphogenetic protein-2 carriers. Int J Pharm. 1999; 1851:51–60. [PubMed: 10425365]
61. Winn SR, Uludag H, Hollinger JO. Carrier systems for bone morphogenetic proteins. Clin Orthop Relat Res. 1999; 367(Suppl):S95–106. [PubMed: 10546639]
62. Genes NG, Rowley JA, Mooney DJ, Bonassar LJ. Effect of substrate mechanics on chondrocyte adhesion to modified alginate surfaces. Arch Biochem Biophys. 2004; 4222:161–167. [PubMed: 14759603]
63. Putnam, C. Protein Calculator. March 28, 2006 August 24, 2010]; Available from: http://www.scripps.edu/~cdputnam/protcalc.html
64. Silva EA, Mooney DJ. Spatiotemporal control of vascular endothelial growth factor delivery from injectable hydrogels enhances angiogenesis. J Thromb Haemost. 2007; 53:590–598. [PubMed: 17229044]
65. Ruppert R, Hoffmann E, Sebald W. Human bone morphogenetic protein 2 contains a heparin-binding site which modifies its biological activity. Eur J Biochem. 1996; 2371:295–302. [PubMed: 8620887]
66. Haidar ZS, Hamdy RC, Tabrizian M. Biocompatibility and safety of a hybrid core-shell nanoparticulate OP-1 delivery system intramuscularly administered in rats. Biomaterials. 2010; 3110:2746–2754. [PubMed: 20044132]
67. Wei G, Jin Q, Giannobile WV, Ma PX. The enhancement of osteogenesis by nano-fibrous scaffolds incorporating rhBMP-7 nanospheres. Biomaterials. 2007; 2812:2087–2096. [PubMed: 17239946]
68. Li B, Yoshii T, Hafeman AE, Nyman JS, Wenke JC, Guelcher SA. The effects of rhBMP-2 released from biodegradable polyurethane/microsphere composite scaffolds on new bone formation in rat femora. Biomaterials. 2009; 3035:6768–6779. [PubMed: 19762079]
69. Brown KV, Li B, Guda T, Perrien DS, Guelcher S, Wenke JC. Improving Bone Formation in a Rat Femur Segmental Defect by Controlling BMP-2 Release. Tissue Eng Part A. 2011

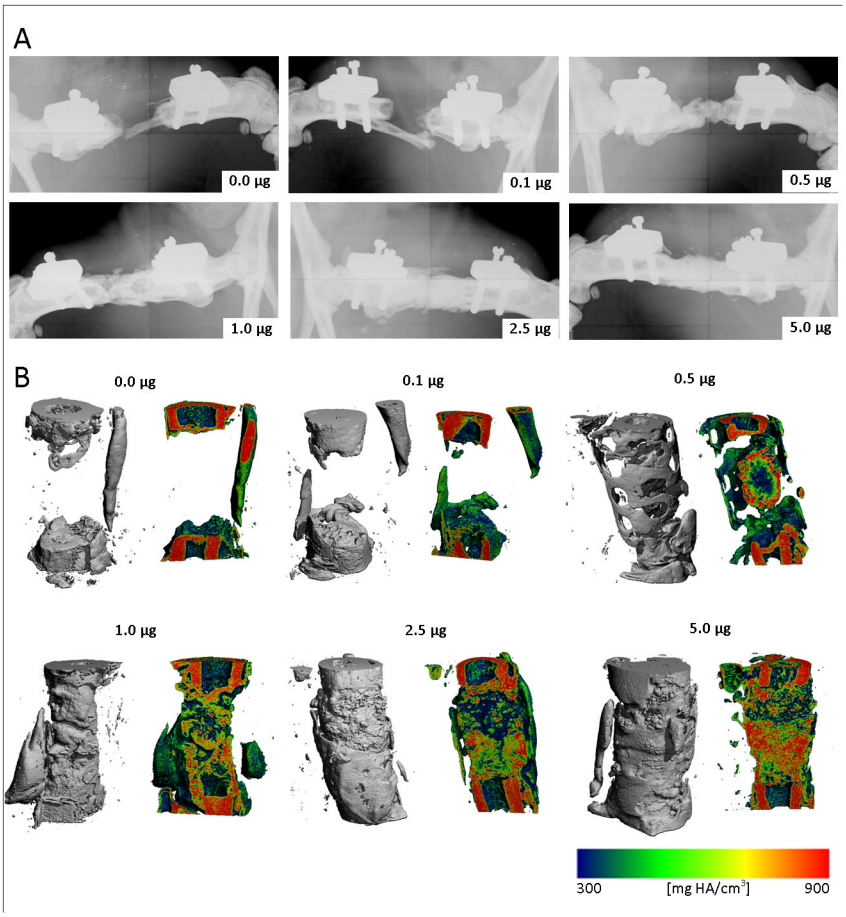

Figure 1.

Representative digital radiographs (A) and microCT reconstructions (B) showing 3-dimensional structure and saggital cross sections illustrating local mineral density mapping. Segmental defects were treated with 0.0, 0.1, 0.5, 1.0, 2.5, and 5.0 μg rhBMP-2, as indicated, delivered in the nanofiber mesh/alginate delivery system.

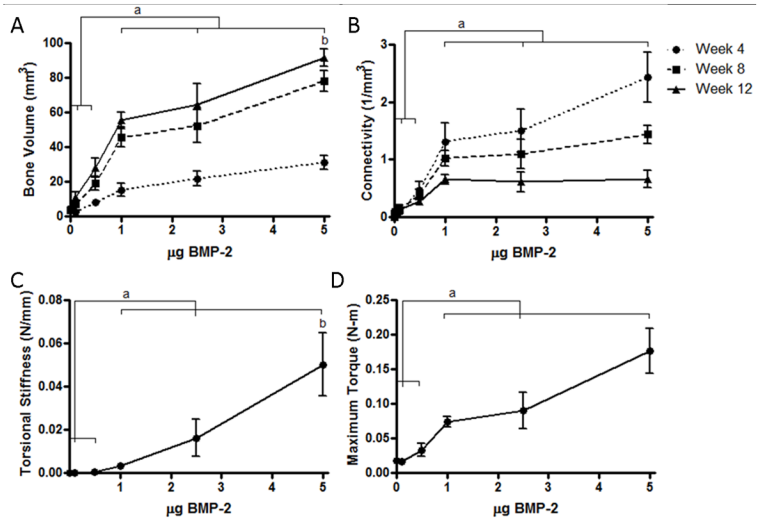

Figure 2.

A, B: MicroCT evaluation of bone volume and connectivity, respectively, as a function of rhBMP-2 dose at week 4 (light dashed lines), week 8 (bold dashed lines), and week 12 (solid lines). Bone volume (A) and connectivity (B) demonstrated nonlinear dose-dependent responses to rhBMP-2, with a reduction in response to increased dose above 1.0 µg. C, D: Postmortem biomechanical properties as a function of rhBMP-2 dose. Torsional stiffness (C) and failure torque (D) continuously increased with increasing dose of rhBMP-2. a: $p < 0.05$ as indicated, b: $p < 0.05$ vs. all other groups.

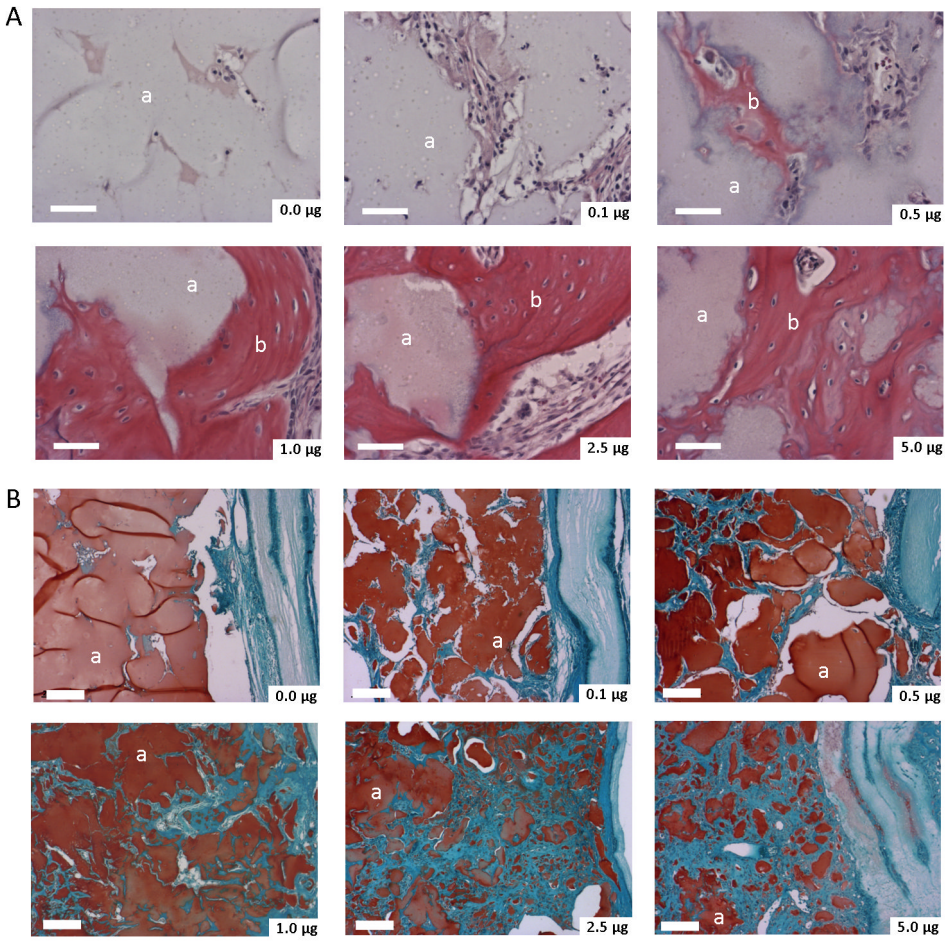

Figure 3.
Week 12 histological staining of saggital sections at each dose of BMP-2, delivered in the mesh/alginate delivery system. H&E staining (A) illustrated bone formation (white arrow) and cellular invasion. Images at 20x, scale bars: 50 μm. Safranin-O/fast green staining at 4x (B) illustrated dose-dependent increases in alginate gel (black arrow) fragmentation and degradation as well as tissue infiltration (fast green counterstain). Images at 4x, scale bars: 200 μm.

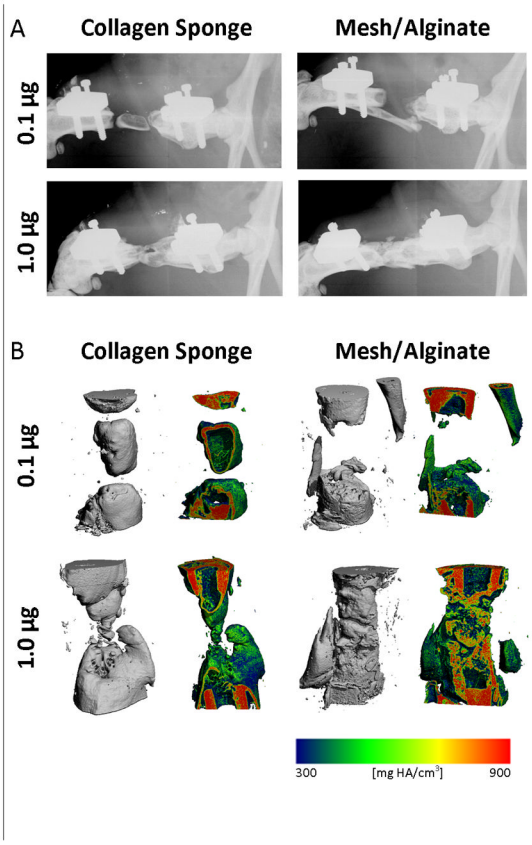

Figure 4.
Week 12 digital radiographs (A) of segmental defects treated with 0.1 or 1.0 µg rhBMP-2, delivered in either collagen sponge or in the nanofiber mesh/alginate delivery system. MicroCT reconstructions (B) and saggital cross sections with local mineral density mapping to illustrate bone formation, defect bridging and tissue maturity.

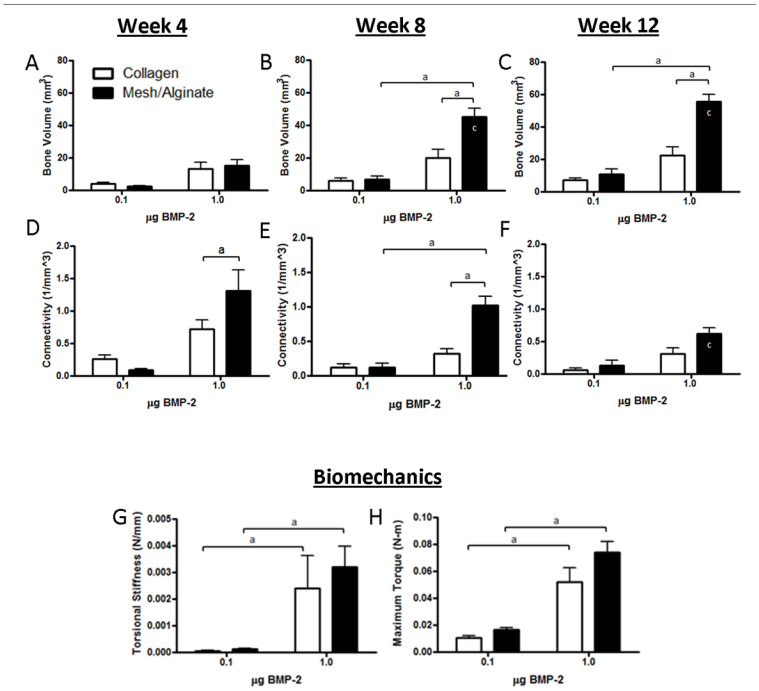

Figure 5.

In vivo microCT quantification of bone volume (A–C) and connectivity (D–E) at week 4 (A, D), week 8 (B, E) and week 12 (C, F) post-surgery. Dark bars represent mesh/alginate delivery system and light bars represent collagen sponge delivery system. Mesh/alginate delivery yielded an early increase in connectivity (D) and conferred a 2.5-fold greater bone volume by week 12 (C) in comparison to collagen sponge delivery. Post-mortem biomechanical testing (G, H) revealed significant dose-dependent increases in stiffness (G) and failure torque (H) but differences between delivery systems were not significant at either dose. a: $p < 0.05$ as indicated, c: $p < 0.05$ vs. same group at week 4.

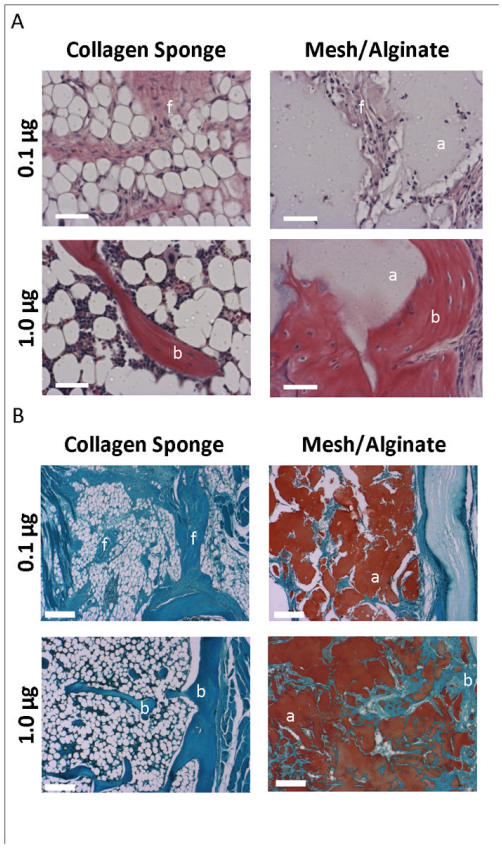

Figure 6.

Week 12 histological staining of saggital sections. H&E staining (A) illustrated bone (b) and fibrous tissue (f) formation and residual alginate (a). Images at 20x, scale bars: 50 μm. Staining with Safranin-O (B) revealed a significant persistence of alginate gel (a) through week 12 in the mesh/alginate group. Large amounts of fibrous tissue (f) were apparent in the collagen sponge group at 0.1 μg, while at 1.0 μg small amounts of trabecular bone (b) and fatty marrow filled the defect. The collagen sponge had entirely absorbed by week 12 in both collagen sponge groups. Images at 4x, scale bars: 200 μm.

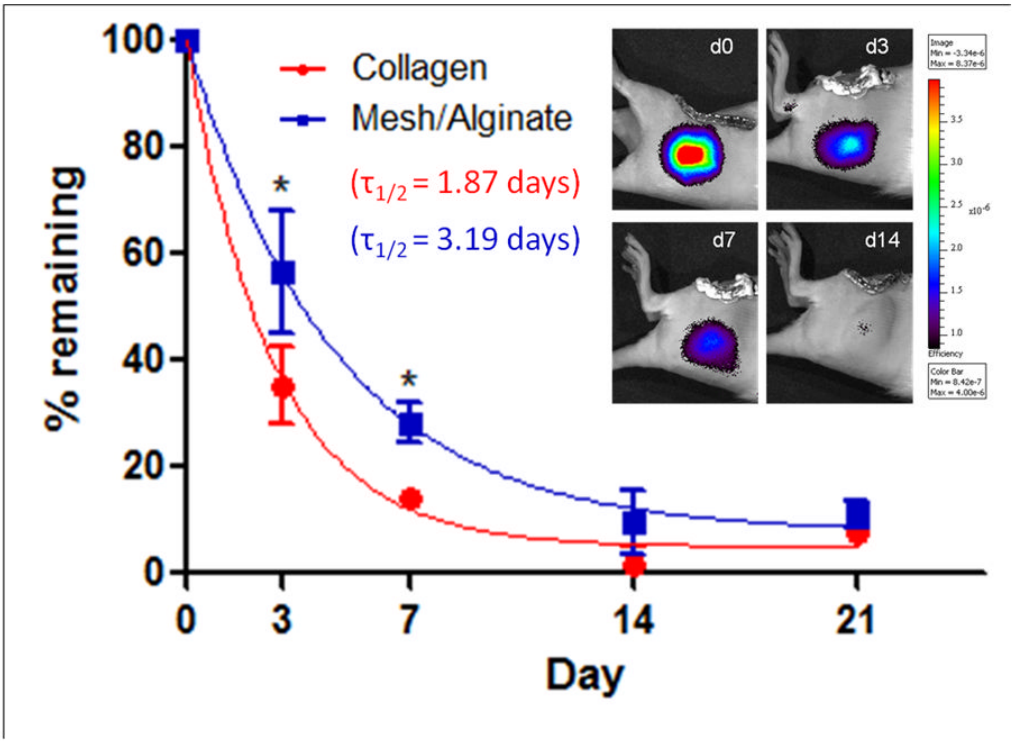

Figure 7.

In vivo tracking of fluorescent tag-labeled rhBMP-2 (inset) over 21 days revealed a significantly elevated protein retention in the mesh/alginate group compared to collagen sponge at day 3 and 7 post-implantation. Solid lines represent curve fit to exponential decay (R^2 = 0.946 and 0.857 for collagen sponge and mesh/alginate groups, respectively). The half life of release was 1.87 days (95% CI: 1.49 to 2.49 days) and 3.19 days (95% CI: 2.23 to 5.59 days), for the collagen sponge and mesh/alginate, respectively.

Table 1

Groups and analyses performed.

Groups		Analysis methods & Sample Sizes				
Dose (μg rhBMP-2)	**Delivery System**	**X-ray**	**MicroCT**	**Mech. Test**	**Histology**	**Protein Release**
0.0	**Mesh/Alginate**	10	10	9	1	
0.1	**Mesh/Alginate**	10	10	9	1	
0.5	**Mesh/Alginate**	10	10	9	1	
1.0	**Mesh/Alginate**	9	9	8	1	
2.5	**Mesh/Alginate**	10	10	9	1	6
5.0	**Mesh/Alginate**	10	10	9	1	
0.1	**Collagen Sponge**	9	9	8	1	
1.0	**Collagen Sponge**	10	10	9	1	
2.5	**Collagen Sponge**	-	-	-	-	6

Table 2

Defect bridging results vs. rhBMP-2 dose delivered in the mesh/alginate system.

Dose	Week 2	Week 4	Week 8	Week 12
0.0 μg	0/10	0/10	1/10	1/10
0.1 μg	0/10	0/10	1/10	3/10
0.5 μg	0/10	0/10	4/10	5/10
1.0 μg	1/9	6/9 *a, b, c*	8/9 *a, b*	9/9 *a, b, c*
2.5 μg	2/10	6/10 *a, b, c*	8/10 *a*	8/10 *a*
5.0 μg	3/10	9/10 *a, b, c*	10/10 *a, b, c*	10/10 *a, b, c*

a $p < 0.05$ vs. 0.0 μg group,

b $p < 0.05$ vs. 0.1 μg group,

c $p < 0.05$ vs. 0.5 μg group.

Table 3

Defect bridging results based on delivery system.

Group	Week 2	Week 4	Week 8	Week 12
M/A 0.1 μg	0/10	0/10	1/10	3/10
Col 0.1 μg	0/9	0/9	0/9	0/9
M/A 1.0 μg	1/9	6/9	8/9	9/9
Col 1.0 μg	1/10	3/10	4/10	6/10 *d*

d $p < 0.05$ vs. collagen 0.1 μg group.